

# NV-like defects more common than four-leaf clovers: A perspective on high-throughput point defect data

Cite as: Appl. Phys. Lett. **127**, 150501 (2025); doi: [10.1063/5.0289896](https://doi.org/10.1063/5.0289896)

Submitted: 10 July 2025 · Accepted: 19 September 2025 ·

Published Online: 14 October 2025



View Online



Export Citation



CrossMark

Joel Davidsson<sup>a)</sup> 

## AFFILIATIONS

Department of Physics, Chemistry and Biology, Linköping University, Linköping, Sweden

<sup>a)</sup> Author to whom correspondence should be addressed: [joel.davidsson@liu.se](mailto:joel.davidsson@liu.se)

## ABSTRACT

Point defect for quantum technologies is an emerging research area, with the nitrogen-vacancy (NV) center in diamond at the forefront. However, how rare are defects with NV-like properties? In this Perspective, I highlight the results of NV-like defects across 33 different materials, revealing that they are more common than finding four-leaf clovers. I also discuss expanding the search criteria to identify other defects relevant to quantum technologies. Utilizing point defect databases will be instrumental in assisting researchers in discovering previously unexplored defects suitable for quantum technologies.

© 2025 Author(s). All article content, except where otherwise noted, is licensed under a Creative Commons Attribution-NonCommercial 4.0 International (CC BY-NC) license (<https://creativecommons.org/licenses/by-nc/4.0/>). <https://doi.org/10.1063/5.0289896>

## I. INTRODUCTION

The nitrogen-vacancy (NV) center is the original defect<sup>1–3</sup> for quantum technologies and continues to be a focus of active research works and applications. It is one of the leading examples of isolated spin defects in solid-state systems, playing a crucial role in the three main areas of quantum technology: computing, communication, and sensing.<sup>4</sup> The robust properties of the NV center have also inspired the development of specific criteria for finding other color centers suitable for quantum technologies. Weber *et al.* outline five requirements for the defect and four for the host materials.<sup>5</sup>

However, the NV center does have its limitations, such as optical emission in the visible range,<sup>1</sup> suffering from spectral diffusion,<sup>6</sup> and a low Debye–Waller factor.<sup>7</sup> While other defects are being explored,<sup>8,9</sup> a key question remains: How rare are defects suitable for quantum technologies with NV-like properties? The answer lies in the high-throughput data.

In order for a defect to be relevant in the realm of quantum technologies, its properties must align with the specific intended application. Each pillar of quantum technologies requires specific defect properties, but they all revolve around a spin that can be initialized, manipulated, and readout. Often high-spin states (triplet or higher) are desirable since the high spin decouples from the electronic background of  $S = 1/2$  and allows for coherent spin control even at zero magnetic field.<sup>10</sup> To find defects that rival the NV center, in this Perspective, the

properties are reduced to three essential ones: defects that are stable with high spin and optical features.

While additional theoretical methods are available to model defects in greater detail,<sup>11</sup> most of these advanced techniques are currently too costly to apply in a high-throughput manner. Moreover, several practical challenges need to be addressed in order to realize unexplored color centers with spin. However, this Perspective does not address these challenges.

In this Perspective, I show that NV-like defects are more common (conservative estimate: about 1 in 500) than finding a four-leaf clover (1 in 5076<sup>12</sup>) when examining the key properties of stability, spin characteristics, and optical features. I also discuss how to relax these criteria to find additional defects suitable for quantum technologies. The outline of the paper is as follows: Sec. II introduces the Automatic Defect Analysis and Qualification (ADAQ) database. I show that the known defects in diamond and 4H-SiC are found in the database. I also provide an example of a predicted defect that has been realized in experiments. Section III shows how NV-like defects are found and their trends across the periodic table. Section IV discusses alternative ways to search for suitable defects beyond NV-like defects. Section V discusses how to improve the data in terms of theoretical approaches and methodologies. Section VI concludes the paper by highlighting the significant opportunity to discover unexplored defects using high-throughput data and discusses strategies to accelerate the search even further.

II. ADAQ

There is an increase in high-throughput calculations and databases for point defects in both bulk<sup>13–15</sup> and 2D materials.<sup>16–19</sup> In this Perspective, the focus is on the ADAQ database. The ADAQ code is the culmination of a series of publications.<sup>20–25</sup> In short, it is an extension of the high-throughput toolkit (*httk*).<sup>26</sup> It uses the Vienna *Ab initio* Simulation Package (VASP)<sup>27,28</sup> with projector augmented wave (PAW)<sup>29,30</sup> pseudopotentials, which in turn perform density functional theory (DFT) calculations. The screening workflow relies on the Perdew, Burke, and Ernzerhof (PBE) functional.<sup>31</sup>

ADAQ automatically generates the initial defect geometries based on symmetry. It can generate arbitrary-sized defect clusters, but the focus is usually on single defects (vacancy, substitutional, and interstitial) and double defects, such as substitutional-vacancy complexes. Each geometry is processed through a screening workflow that calculates different charges and spin states, focusing initially on the neutral charge state. The inverse participation ratio (IPR)<sup>32</sup> is used to identify defect states in the bandgap. Additional charge ( $\pm 1$ ) and spin states are calculated when possible. The calculation of alternative spin states is key for determining the most energetically stable spin state. Finally, an excitation is calculated using the Delta Self-Consistent Field ( $\Delta$ SCF) method.<sup>33</sup> All calculated states, along with properties like formation energies, structural changes (such as  $\Delta Q$ ), and optical attributes like zero phonon line (ZPL) and transition dipole moment (TDM),<sup>23</sup> are stored in a database for further filtering of relevant defects. Good optical features are characterized by ZPL values within an appropriate range, a large TDM, and a small  $\Delta Q$ .

In other high-throughput studies, the term *defect* is often loosely defined and occasionally includes different charge states of the same defect geometry. While slight relaxations exist between the various charge states of a defect, in my opinion, the defect geometries are too similar to consider them separate defects. Therefore, from now on, when I refer to a *defect* or count them, I specifically refer to the initial defect geometry. For instance, in 4H-SiC, there are two symmetry-inequivalent vacancy positions; these are counted as two distinct defects or defect types. It is crucial to note that an entry in the database is uniquely defined by the combination of defect, charge, and spin states, which adds an important layer of specificity. This discussion highlights the importance of standardizing the nomenclature related to defects, similar to the standardization achieved for materials with OPTIMADE.<sup>34</sup>

A. Defect hull

Materials are ordered by thermodynamic stability using the convex hull. Analogously, the concept of the defect hull was introduced to order the defects based on their stability.<sup>24,35</sup> The defect hull consists of the point defects with the lowest formation energy for a given stoichiometry and Fermi energy. Hence, different defects can span the hull for the same stoichiometry, such as the positive charge state of a carbon vacancy-antisite pair and the negative charge state of a silicon vacancy for the same stoichiometry (one missing silicon) in 4H-SiC.<sup>24</sup> This result means that the defect hull can not only consist of complexes (double defects) but also single defects. In general, calculating single defects is a good starting point, but the earlier example highlights an important exception to include complexes. Furthermore, the ordering within each stoichiometry of the defect hull is independent of the chemical potentials. This attribute means that rich or poor phases do not affect any searches. After a defect is found, the chemical

potentials can be optimized to tune the absolute formation energy. The defect hull concept has proven instrumental in finding known defects for quantum technologies. It will also assist in identifying relevant dopants for energy-related applications, such as power converters.

B. Known defects

Let us start by searching for known defects in diamond in the ADAQ database. Apart from the NV center, the XV (X = Si, Ge, Sb, Pb) centers have recently attracted attention for quantum technologies.<sup>36</sup> These defects are on the defect hull with the known charge and spin states, see Table I. Two key points are worth noting. First, the PBE functional underestimates the ZPLs by about 0.25 eV compared to experimental values.<sup>37</sup> This underestimation primarily depends on the material, and the HSE functional yields ZPLs that closely agree with experimental results. Second, ZPLs are missing for the Si, Ge, and Sn defects. This result is due to one of the defect states being below the valence band, and ADAQ only calculates excitations between states within the bandgap, as discussed more in Sec. V A. However, as the size of the dopant atom increases, this defect state moves into the bandgap, and ADAQ captures the transition for the PbV center. This outcome is consistent across different functionals, with the HSE functional also exhibiting the same trend.<sup>38</sup>

Next, we will examine known defects in 4H-SiC. The 4H polytype has atoms with different symmetries, meaning the same defect can exist in multiple configurations. One of these configurations will be located on the defect hull, while the others will be positioned at a distance from the hull ( $\epsilon$ ). Table II shows the results for the divacancy and silicon vacancy. Again, ADAQ finds the known charge and spin states, and the ZPLs are underestimated by about 0.2 eV in this case.<sup>21,22,25</sup> Notably, some configurations, such as the *kk* configuration, show better agreement with experimental results due to error cancellation.<sup>25</sup> For the silicon vacancy in the *k* configuration, one of the defect states lies below the valence band, causing a missing ZPL. In contrast to the previous discussion on defect states below the valence band, this instance can be solved by converging the calculation more thoroughly. However, the low settings in the screening workflow are required to process the vast amount of defects effectively.

There is a difference in formation energy between the configurations, which is reflected in the distance to the defect hull. For the divacancy, the *kk* configuration is on the defect hull, but the other configurations are also observed experimentally. The *hk* configuration is 115 meV higher in energy than the *kk* configuration, indicating that some defects above the defect hull can be observed. For now, let us set the distance to the hull to 30 meV and discuss this further in Sec. IV A.

TABLE I. ADAQ data for known defects in diamond.

Defect	On defect hull	Charge	Spin	Calc. ZPL (eV)	Exp. ZPL (eV)
NV	Yes	−1	1.0	1.700	1.945 <sup>1</sup>
SiV	Yes	−1	0.5	<sup>a</sup>	1.680 <sup>36</sup>
GeV	Yes	−1	0.5	<sup>a</sup>	2.060 <sup>36</sup>
SnV	Yes	−1	0.5	<sup>a</sup>	2.000 <sup>36</sup>
PbV	Yes	−1	0.5	2.122	2.384 <sup>36</sup>

<sup>a</sup>Missing values, see main text for further details.

18 October 2025 14:39:24

TABLE II. ADAQ data for known defects in 4H-SiC.  $\epsilon$  is the distance to the defect hull.

Defect	Configuration	$\epsilon$ (meV)	Charge	Spin	Calc. ZPL (eV)	Exp. ZPL (eV)
$V_{Si}V_C$	$hh$	20	0	1.0	0.992	1.095 <sup>39</sup>
$V_{Si}V_C$	$hk$	115	0	1.0	1.005	1.150 <sup>39</sup>
$V_{Si}V_C$	$kh$	68	0	1.0	0.961	1.119 <sup>39</sup>
$V_{Si}V_C$	$kk$	0	0	1.0	1.012	1.096 <sup>39</sup>
$V_{Si}$	$h$	0	−1	1.5	1.270	1.440 <sup>40</sup>
$V_{Si}$	$k$	9	−1	1.5	<sup>a</sup>	1.353 <sup>40</sup>

<sup>a</sup>Missing values, see main text for further details.

I would like to make two final remarks about the results in 4H-SiC. First, according to the ADAQ database, the carbon vacancy-antisite pair (CAV) is not related to the AB lines, which is also supported by higher-order calculations (GW).<sup>41</sup> Instead, the CAV is predicted to emit close to the telecom bands.<sup>41</sup> Finally, while searching for the silicon vacancy in the ADAQ database, additional defects with the same spin and similar ZPLs were also found. These defects are the modified silicon vacancies, which consist of a silicon vacancy with a carbon antisite as a second-nearest neighbor. These defects were identified through experiments, demonstrating the predictive power of high-throughput methods.<sup>35</sup>

III. NV-LIKE DEFECTS

This section highlights various host materials for quantum technologies and their number of defects, outlines criteria for NV-like defects, and details several selected defects discovered through the high-throughput approach.

A. Hosts

Research continues on defects in traditional materials for quantum technologies like diamond and SiC. ADAQ has processed 8450 single and double defects in diamond<sup>37,42</sup> and 60 081 single and double defects in 4H-SiC.<sup>24,35,43</sup> While both diamond and SiC are great hosts, other materials with longer coherence times have also been suggested. Kanai *et al.* ranked the materials in the Materials Project<sup>44</sup> based on their coherence time and found that oxides are at the top.<sup>45</sup> Notably, calcium oxide (CaO) ranks third among all computed materials (first if materials with d- and f-elements are excluded). Magnesium oxide (MgO) shares a similar ranking to diamond. Single and double defects were calculated in these materials, resulting in 9077 defects in CaO<sup>46</sup> and 2917<sup>48</sup> defects in MgO.<sup>47,48</sup> Additionally, Ferrenti *et al.* reduced the Materials Project database<sup>44</sup> to 541 materials with suitable properties (stable, low number of nuclear spin isotopes, bandgap larger than 1.1 eV) for hosting quantum defects.<sup>49</sup> Groppfeldt *et al.* further reduced this list and calculated 17 710 single defects in 29 materials.<sup>50</sup> All materials were doped with s- and p-elements from H to Bi. In total, about 100 000 defects (initial defect geometries) have been processed by ADAQ, which can now be filtered for quantum technology applications.

B. Search criteria

In this Perspective, NV-like defects are found with the following search criteria. The defect should be

- stable within 30 meV of the defect hull ( $\epsilon < 30$  meV),
- with a spin of 1 or greater ( $S \geq 1$ ),
- and an optical signal (ZPL  $> 0.5$  eV and TDM  $> 3$  Debye).

In Sec. IV, I discuss what happens if we relax these search criteria.

C. Defects

This search yields 287 NV-like defect entries across 33 materials. These are presented in Fig. 1. It is worth noting that some of these results include duplicates (when removed, 180 defects remain), as the initial structures can relax into the same configuration. Many of the filtered defects are challenging to realize because they involve second-nearest neighbor complexes. Finally, we have not ranked these defects to determine whether they are superior to the NV center, although 111 have a Debye–Waller factor (calculated using the one-phonon approximation) larger than 3%. Nonetheless, while NV-like defects are rare, they are not exceptionally rare. The data indicate that it is easier to find an NV-like defect<sup>51</sup> than a four-leaf clover.<sup>12</sup> Several defects stand out and have been selected for further characterization, with results in Table III.

Apart from the NV center in diamond, other defects exhibit similar properties. Among the various, XV defects are the group 13 vacancy clusters, which have been suggested previously,<sup>53</sup> but also the LiV defect in the positive charge state. Moreover, the group 1 substitutionals also have high spins (spin-3/2 in neutral charge state) and great optical features. Here, Davidsson *et al.* focused on the Na<sub>C</sub> that has NV-like properties in two charge states, highlighting that one defect can have multiple charge and spin states with NV-like properties. Both charge states of Na<sub>C</sub> have a lower ZPL and lower  $\Delta Q$  compared to the NV center.<sup>37</sup>

In 4H-SiC, the nitrogen-vacancy (NV) center is also present, as previously established.<sup>54</sup> However, the high-throughput search identified four additional XV defects that are listed in Table III. As the group is changed, the charge state with NV-like properties also changes. Specifically, O and S defects in the neutral charge state have NV-like properties, whereas F and Cl need to be in the positive charge state. The oxygen vacancy (OV) defect was presented by a separate research group in close connection with the ADAQ results.<sup>55</sup> Using a high-throughput method enabled the full characterization of the defect space and the identification of the full suite of NV-like defects in 4H-SiC. Bulancea-Lindvall *et al.* focused on the ClV defect in more detail, as it is predicted to have a ZPL in the telecom band.<sup>43</sup>

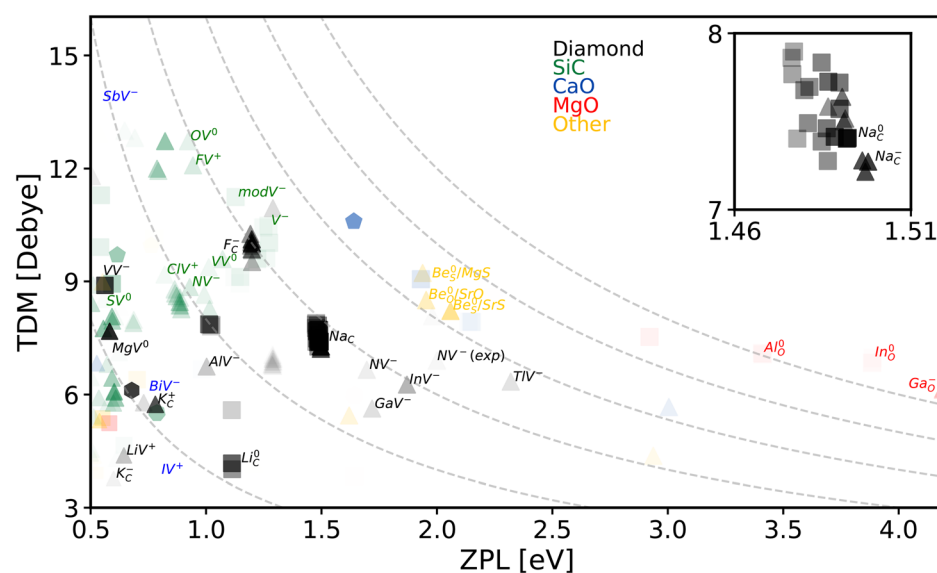


**FIG. 1.** ADAQ (PBE) results for defects that fulfill the search criteria. Near the center, a point shows the experimental characteristics of the NV center. The corners of the marker indicate the stable ground state; for instance, a triangle represents a triplet ground state. The size of each marker corresponds to the radiative lifetime (larger markers correspond to faster rates), while the opacity reflects the Debye-Waller factor. V represents vacancy. Guidelines follow  $1/ZPL$  curves.<sup>24</sup> The inset shows Frenkel pairs ( $\text{In}_{\text{Na}}\text{V}_{\text{C}}$ ) that relaxed into the Na substitutional ( $\text{Na}_{\text{C}}$ ).

So far, we have examined conventional covalent materials, such as diamond and SiC, concerning color centers with spin. Now, we shift to oxides, which are predicted to have longer coherence times, starting with CaO. Again, a class of defects with NV-like properties was found, even though this material is more ionic than previous materials. The XV defects are mostly found in group 15 of the periodic table, where P, As, Sb, and Bi dopants in the negative charge state exhibit NV-like properties. However, since P and As have two local minima, they are excluded from our current discussion. In group 17, the I dopant in the positive charge state also has NV-like properties. In group 16, no NV-like defects have been observed due to the negative U behavior of the XV defects, i.e., the neutral charge state is unstable. Furthermore, the BiV defect also gives rise to a clock transition, where the avoided spin states increase the coherence time by eliminating the first-order decoherence term.<sup>46</sup> This result raises an open question: How common are clock transitions among color centers?

MgO also has the same defect suite as CaO. However, it also has a unique NV-like defect, the nitrogen interstitial combined with a magnesium vacancy.<sup>47</sup> In this defect, the N binds to O, forming a dimer. This example illustrates the importance of considering more complicated defect structures, as the single defect ( $\text{N}_{\text{Mg}}$ ) has an energy approximately 1.5 eV higher. Although oxides are predicted to have better coherence times, other properties might be worse. A notable difference in both MgO and CaO, when compared to diamond and SiC, is the larger  $\Delta Q$ . The ionic nature, materials with lower stiffness, and defects containing vacancies contribute to the larger  $\Delta Q$ , which will limit the Debye-Waller factor. Nevertheless, there may be potential for material engineering to enhance the Debye-Waller factor. Alternatively, other readout mechanisms may be more suitable for these defects, as discussed in Sec. IV C.

Finally, Groppfeldt *et al.* studied single defects in 29 host materials using ADAQ and found 13 NV-like single defects with a Debye-Waller factor  $>1\%$ . Among these defects, three were Be substitutionals ( $\text{Be}_{\text{S}}$  in SrS,  $\text{Be}_{\text{S}}$  in MgS,  $\text{Be}_{\text{O}}$  in SrO).<sup>50</sup> These defects are also found in more ionic materials but still have reasonable  $\Delta Q$  comparable to those in SiC and diamond. This finding emphasizes that alternative materials

can host NV-like defects with properties on par with the NV center in diamond.

## D. Trends

Figure 2 illustrates trends in high-throughput data for NV-like defects. First and foremost, the NV center is found in various materials, including diamond, SiC, and MgO. Although the form and stoichiometry of the NV center in MgO differ from those in diamond, it still involves a nitrogen atom and a vacancy. Furthermore, in certain instances, it is possible to replace nitrogen, as demonstrated by the XV defects ( $X = \text{O}, \text{S}, \text{F}, \text{Cl}$ ) in SiC, and still retain the NV-like properties. Similar trends can be observed in diamond, although they are not as extensive. The neutral OV also exists in diamond, as predicted in earlier works.<sup>56,57</sup> In addition, the ADAQ data suggest that the negative charge state of OV has spin-3/2. Moreover, the FV in diamond follows the trend with a spin-1 ground state in the positive charge state. It also has a spin-2 ground state in the negative charge state, although additional data are needed to confirm this.

These defects are primarily found within the same part of the periodic table, mainly along the rows. There are also trends within the groups; for example, the group 13 vacancy clusters in diamond are one example of predicted defects.<sup>53</sup> Recent DFT modeling of these defects further reinforces the notion that AlV, GaV, and InV are ready for experimental verification.<sup>58</sup> Additionally, the XV defects ( $X = \text{Sb}, \text{Bi}, \text{I}$ ) in CaO and MgO also have NV-like properties.

These examples are taken from the p-block of the periodic table, where the defects are primarily substitutional-vacancy complexes. However, there are also examples in the s-block of substitutional defects. For example, group 1 substitutionals (Li, N, K, and Rb) in diamond also have NV-like properties.<sup>37</sup> Additionally, Beryllium, which belongs to group 2, is found in materials such as SrS, MgS, and SrO.<sup>50</sup> This result shows that defect trends exist across different materials. As long as the defect states remain within the bandgap and the material does not change significantly, the properties of the impurity are preserved. The results depicted in Fig. 2 demonstrate the presence of



**TABLE III.** Selected NV-like defects from the ADAQ database. Found using the NV-like search criteria listed in the text. V indicates vacancy. Added the NV center as a reference.

Host	Defect (configuration)	Charge	Spin	ZPL (eV)	TDM (debye)	$\Delta Q$ (amu <sup>1/2</sup> Å)	Note
Diamond	NV	−1	1.0	1.70	6.66	0.56	ADAQ results <sup>37</sup>
				2.00	6.92	0.71	HSE results <sup>7,46</sup>
	Li <sub>C</sub> V <sub>C</sub>	+1	1.0	0.64	4.38	0.41	ADAQ results <sup>37</sup>
	Li <sub>C</sub>	0	1.5	1.11	4.17	0.21	ADAQ results <sup>37</sup>
	K <sub>C</sub>	−1	1.0	0.59	3.77	0.96	ADAQ results <sup>37</sup>
	K <sub>C</sub>	+1	1.0	0.78	5.74	0.24	ADAQ results <sup>37</sup>
	Na <sub>C</sub>	0	1.5	1.49	7.41	0.16	ADAQ results <sup>37</sup>
				1.59	6.8	0.52	HSE results <sup>37</sup>
	Na <sub>C</sub>	−1	1.0	1.50	7.27	0.15	ADAQ results <sup>37</sup>
				1.68	6.6	0.69	HSE results <sup>37</sup>
4H-SiC	N <sub>C</sub> V <sub>Si</sub> ( <i>hh</i> )	−1	1.0	0.93	8.85	0.59	ADAQ results <sup>43</sup>
	O <sub>C</sub> V <sub>Si</sub> ( <i>hh</i> )	0	1.0	1.07	9.59	0.63	ADAQ results <sup>43</sup>
				1.24	10.42	0.79	HSE results <sup>52</sup>
	S <sub>C</sub> V <sub>Si</sub> ( <i>hh</i> )	0	1.0	0.61	8.07	0.86	ADAQ results <sup>43</sup>
				0.67	9.42	1.02	HSE results <sup>52</sup>
	F <sub>C</sub> V <sub>Si</sub> ( <i>hk</i> )( <i>hh</i> )	+1	1.0	0.94	12.08	0.53	ADAQ results <sup>43</sup>
				1.26	10.50	1.08	HSE results <sup>52</sup>
	Cl <sub>C</sub> V <sub>Si</sub> ( <i>hh</i> )	+1	1.0	0.82	9.18	0.83	ADAQ results <sup>43</sup>
				0.93	9.99	0.96	HSE results <sup>43</sup>
CaO	Sb <sub>Ca</sub> V <sub>O</sub>	−1	1.0	0.54	13.8	4.39	ADAQ results <sup>46</sup>
				0.53	34.7	5.10	HSE results <sup>46</sup>
	Bi <sub>Ca</sub> V <sub>O</sub>	−1	1.0	0.74	5.99	5.05	ADAQ results <sup>46</sup>
				0.76	10.8	6.22	HSE results <sup>46</sup>
	I <sub>Ca</sub> V <sub>O</sub>	+1	1.0	0.79	3.72	3.20	ADAQ results <sup>46</sup>
				0.78	41.8	5.49	HSE results <sup>46</sup>
MgO	Int <sub>N</sub> V <sub>Mg</sub>	−1	1.0	2.19	0.66 <sup>a</sup>	1.95	ADAQ results <sup>47</sup>
				3.19	0.17	3.37	Hybrid TDDFT results <sup>47</sup>
SrS	Be <sub>S</sub>	0	1.0	2.06	8.22	0.55	ADAQ results <sup>50</sup>
MgS	Be <sub>S</sub>	0	1.0	1.94	9.22	0.65	ADAQ results <sup>50</sup>
SrO	Be <sub>O</sub>	0	1.0	1.95	8.51	0.67	ADAQ results <sup>50</sup>

<sup>a</sup>No TDM restriction in search.

NV-like defects throughout the periodic table. Note that the d-block is currently unrepresented, as no defects involving d-elements have been calculated. However, based on the trends observed in the s- and p-blocks, it is probable that many NV-like defects also exist in the d-block.

IV. OTHER SEARCHES

How similar does a defect need to be to the NV center in order to be considered useful? It is possible to relax certain criteria. In this section, we will examine each criterion used to identify NV-like defects to explore other potential ways to discover interesting defects.

A. Defect hull

The stability of defects is a crucial factor to consider. The exact distance to the defect hull remains a topic of discussion. For instance,

as indicated for the divacancy in Table II, the distance can exceed 0.1 eV, yet it can still be realized experimentally. Therefore, a small buffer from the defect hull is necessary. Another reason for having a buffer is that the spin states may be close in energy, and higher-order calculations could shift these states to favor one over the others. A buffer of 0.1 eV may be sufficient for the PBE data, and it is discussed more in Sec. V.

There is also the remote possibility that defects are metastable. They could get stuck in the local geometry and locked within the crystal. In this context, diffusion barriers play a crucial role, and they are also discussed in Sec. V. Increasing the distance to the defect hull to 1 eV or greater makes it possible to include metastable defects. However, additional checks must be performed to ensure that no other defects are closer to the defect hull, neither in terms of lower-lying spin states of the same defect nor a relaxation pathway that could transform

Group →	1	2	3	4	5	6	7	8	9	10	11	12	13	14	15	16	17	18		
↓ Period																				
1	1 H	diamond												diamond		SiC		2 He		
2	3 Li	4 Be	MgS, SrS, SrO												5 B	6 C	7 N	8 O	9 F	10 Ne
3	11 Na	12 Mg													13 Al	14 Si	15 P	16 S	17 Cl	18 Ar
4	19 K	20 Ca	21 Sc	22 Ti	23 V	24 Cr	25 Mn	26 Fe	27 Co	28 Ni	29 Cu	30 Zn	31 Ga	32 Ge	33 As	34 Se	35 Br	36 Kr		
5	37 Rb	38 Sr	39 Y	40 Zr	41 Nb	42 Mo	43 Tc	44 Ru	45 Rh	46 Pd	47 Ag	48 Cd	49 In	50 Sn	51 Sb	52 Te	53 I	54 Xe		
6	55 Cs	56 Ba		72 Hf	73 Ta	74 W	75 Re	76 Os	77 Ir	78 Pt	79 Au	80 Hg	81 Tl	82 Pb	83 Bi	84 Po	85 At	86 Rn		
7	87 Fr	88 Ra		104 Rf	105 Db	106 Sg	107 Bh	108 Hs	109 Mt	110 Ds	111 Rg	112 Cn	113 Nh	114 Fl	115 Mc	116 Lv	117 Ts	118 Og		
																	CaO		MgO	

**FIG. 2.** Trends of NV-like defects across the periodic table are represented as follows: defects in diamond are marked in black, defects in SiC in green, CaO in blue, and MgO in red. Defects in MgS, SrS, and SrO are marked in yellow. Dashed lines represent defects with uncertain trends.

the metastable defect to another more stable defect. Metastable defects for quantum applications are highly unlikely, but further studies are needed.

Finally, the defect hull criterion requires further refinement. The current criteria, which emphasize stability for any Fermi level, may be overly broad. Improving this approach involves considering the actual Fermi level and the feasibility of doping to achieve it. Additionally, it should also assess whether the defect remains stable over a wide or narrow range of Fermi levels. Updating this criterion could help narrow down the list of defects more efficiently.

## B. Spin

So far, the search criterion has been for spin-1 or higher. The ratio of triplet to singlet and doublet ground states depends on the host material. Traditional viewpoints emphasize symmetry. If the symmetry of the host material drops below space group 74, the crystal no longer has any degenerate states. Consequently, the availability of triplet ground states should depend on the symmetry of the host materials. Generally, high-symmetry materials should have a higher incidence of high-spin ground states. However, while it is less likely to find high-spin ground states in low-symmetry crystals, it is not impossible. Without degenerate levels, high-spin states occur when the exchange coupling between electrons in different defect states exceeds the single-particle energy difference between those states.<sup>10</sup> For example, the silicon vacancy in SiC has spin-3/2 even though the crystal has lower symmetry without triple degenerate states. Furthermore, unexpectedly, many spin defects with high spin were found in systems with low symmetry.<sup>50</sup> Additionally, low-symmetry environments can create defects with anisotropic g-factors that offer faster driving speeds and lower decoherence.<sup>4</sup>

While triplet or higher spin ground states are preferable, a doublet ground state may be sufficient. For instance, the XV defects—where X represents Si, Ge, Sn, or Pb in diamond—have received significant

attention, and they have a doublet ground state in the negative charge state.<sup>36</sup> If we broaden the spin criterion to  $S \geq 1/2$ , the number of defects increases dramatically since about half of all defects in a material have a doublet ground state (about 46% in 4H-SiC<sup>24</sup>) regardless of the symmetry of the host.

## C. Readout

Optical readout is generally preferred in many applications.<sup>4</sup> For effective optical readout, it is important to have a bright ZPL and a large Debye–Waller factor. Additionally, considering relaxation processes in the excited state is crucial, both for estimating the Debye–Waller factor and because certain defects exhibit significant relaxation in the excited state. For example,  $O_{Si}$  in 4H-SiC has an absorption of 1.76 eV, whereas the ZPL is around 0.8 eV.

However, electrical or mechanical readout offers alternative control possibilities, as demonstrated for the NV center in diamond.<sup>59</sup> Hence, the requirements of a bright ZPL and a large Debye–Waller factor may not be necessary in all cases; it depends on the application. In quantum communication, where flying qubits are essential, optical readout is, indeed, important. However, for quantum computing or sensing, alternative readout protocols may be more beneficial. Therefore, it is necessary to update databases to filter for the relevant properties that help identify defects suitable for electrical or mechanical readout.

## V. IMPROVING THE DATA

Searches have been applied to the screening data, which is produced with the PBE functional. The results obtained from this filtering process are only as reliable as the data itself. The PBE functional has known weaknesses, including smaller band gaps and possible incorrect ordering of spin states. There is, of course, a risk that we overlook interesting systems due to these errors. This challenge is common in all high-throughput approaches, and the goal is to mitigate these

errors. Despite utilizing relatively low convergence settings and the PBE functional, intriguing defects have still been identified in the data. It is essential to validate every prediction derived from the screening data using higher-order methods.

With this context, let us discuss how to improve the screening data. I see three possible avenues for enhancement: (i) Implementing a HSE screening workflow that will improve the bandgap and relative spin state energies. However, since it is more expensive, it is necessary to rely on geometries that are relaxed with the PBE functional. (ii) Expanding the database with additional properties is a logical next step. Among the top priorities are spin-related properties, such as zero-field splitting and hyperfine coupling parameters. Another important aspect to consider is the various rates for spin relaxation pathways. It would be beneficial to have a rapid method for determining whether a defect has an optical cycle and if its spin can be initialized. Currently, existing methods are too expensive to implement in a high-throughput workflow. (iii) Instead of pursuing more accurate functionals and methods, we could focus on developing faster methods at the PBE level, which would also enhance the screening data. There are many defect systems left to explore. If we had faster methods, we could evaluate more defects, larger complexes, more charge states, and more excitations. Additionally, we should investigate co-doping strategies, as current defect analyses typically involve only one external dopant, rather than mixtures. Combining different dopants may be necessary to realize specific defects in the desired charge state. Furthermore, calculating energy barriers using nudge-elastic band methods and addressing defects in stacking faults<sup>60</sup> also require faster methods. Using the SCAN functional could improve performance in both areas, as demonstrated for NV-like defects in 4H-SiC, where many properties align more closely with the HSE results while maintaining a similar computational cost to the PBE functional.<sup>52</sup>

### A. Symmetry analysis

In parallel to updating the computational methods, there is also a need to update the algorithms used for identifying defects and selecting transitions. Currently, the ADAQ screening workflow selects only one excitation per defect, potentially overlooking important excitations between defect states within the bandgap or selecting forbidden transitions. One potential solution is to incorporate symmetry analysis. The recently published code, ADAQ-SYM, calculates the character of defect states and determines the selection rules for any given defect.<sup>61</sup> This approach was verified on the SiV in diamond, where the correct excitation was identified. The intention is to apply ADAQ-SYM to the ADAQ database to search for additional ZPLs that may have been previously overlooked.

The selection rules are also valuable for gaining a deeper understanding of the defects and may allow for the optical selection of which defect to excite. For the divacancy and NV center in SiC, it is possible to avoid exciting the high-symmetry configurations, which leads to an increase in the ODMR contrast for the low-symmetry configurations.<sup>62</sup> However, this possibility is not available for all defects and depends on the structure and symmetry of the defect.

Understanding the symmetry properties is crucial not only for determining transitions but also for gaining a deeper insight into the defects themselves. Moreover, the symmetry knowledge is a step toward generating many-body diagrams and exploring strain deformations.

## VI. CONCLUSION

High-throughput data have identified and predicted defects for quantum technologies, with many unexplored defects that may rival the NV center in diamond. Numerous defects are awaiting further theoretical investigation and experimental realization. On the theoretical side, advancements in theoretical characterization and more data are needed to guide experimental efforts. Currently, the ADAQ database allows users to filter defects but lacks recipes for creating them. Improved methods could provide guidelines on sample preparation, doping concentrations, and annealing conditions for generating or optimizing specific defects. On the experimental side, I would like to see a structured approach for generating point defects, ideally with an automated setup that implants, anneals, and measures multiple samples while documenting each step of the process in a public database.

We are at the beginning of the research field dedicated to point defects for quantum technologies, which has the potential to become the dominant quantum technology. There will not be a single defect system for all applications; rather, multiple defect systems tailored for specific applications. Although a significant amount of work is required to bring defects to the same level as the NV center, existing databases currently provide many promising defects for further study. The most significant defects may still be undiscovered, and the choice of host material remains undecided. However, with more systematic data collection and analysis, we will come closer to identifying the optimal defects, and I expect that more NV-like defects will be identified in the future.

## ACKNOWLEDGMENTS

The author thanks Oscar Bulancea-Lindvall, Rickard Armiento, and Igor Abrikosov for valuable discussions and insights on the manuscript.

The author acknowledges funding from the Swedish Research Council (VR) under Grant No. 2022-00276 and the Knut and Alice Wallenberg Foundation through the WBSQD2 project (Grant No. 2018.0071).

Most of the ADAQ computations discussed in this paper were enabled by resources provided by the National Academic Infrastructure for Supercomputing in Sweden (NAISS), partially funded by the Swedish Research Council through grant agreement no. 2022-06725.

## AUTHOR DECLARATIONS

### Conflict of Interest

The author has no conflicts to disclose.

### Author Contributions

**Joel Davidsson:** Conceptualization (lead); Formal analysis (lead); Resources (lead); Visualization (lead); Writing – original draft (lead); Writing – review & editing (lead).

## DATA AVAILABILITY

The data that support the findings of this study are openly available in the ADAQ database (<https://defects.anyterial.se/>).

## REFERENCES

- <sup>1</sup>G. Davies and M. F. Hamer, "Optical studies of the 1.945 eV vibronic band in diamond," *Proc. Math. Phys. Eng. Sci.* **348**, 285 (1976).
- <sup>2</sup>A. Gruber, A. Dräbenstedt, C. Tietz, L. Fleury, J. Wrachtrup, and C. V. Borczyskowski, "Scanning confocal optical microscopy and magnetic resonance on single defect centers," *Science* **276**, 1212 (1997).
- <sup>3</sup>M. W. Doherty, N. B. Manson, P. Delaney, F. Jelezko, J. Wrachtrup, and L. C. Hollenberg, "The nitrogen-vacancy colour centre in diamond," *Phys. Rep.* **528**(1), 1 (2013).
- <sup>4</sup>G. Wolfowicz, F. J. Heremans, C. P. Anderson, S. Kanai, H. Seo, A. Gali, G. Galli, and D. D. Awschalom, "Quantum guidelines for solid-state spin defects," *Nat. Rev. Mater.* **6**, 906 (2021).
- <sup>5</sup>J. R. Weber, W. F. Koehl, J. B. Varley, A. Janotti, B. B. Buckley, C. G. V. de Walle, and D. D. Awschalom, "Quantum computing with defects," *Proc. Natl. Acad. Sci. U. S. A.* **107**, 8513 (2010).
- <sup>6</sup>B. McCullian, H. Cheung, H. Chen, and G. Fuchs, "Quantifying the spectral diffusion of n-v centers by symmetry," *Phys. Rev. Appl.* **18**, 064011 (2022).
- <sup>7</sup>A. Alkauskas, B. B. Buckley, D. D. Awschalom, and C. G. Van de Walle, "First-principles theory of the luminescence lineshape for the triplet transition in diamond NV centres," *New J. Phys.* **16**, 073026 (2014).
- <sup>8</sup>D. DiVincenzo, "Better than excellent," *Nat. Mater.* **9**, 468 (2010).
- <sup>9</sup>G. Zhang, Y. Cheng, J.-P. Chou, and A. Gali, "Material platforms for defect qubits and single-photon emitters," *Appl. Phys. Rev.* **7**, 031308 (2020).
- <sup>10</sup>L. C. Bassett, A. Alkauskas, A. L. Exarhos, and K.-M. C. Fu, "Quantum defects by design," *Nanophotonics* **8**, 1867 (2019).
- <sup>11</sup>A. Gali, "Ab initio theory of the nitrogen-vacancy center in diamond," *Nanophotonics* **8**, 1907 (2019).
- <sup>12</sup>See <https://news.uga.edu/four-leaf-clover-spotting/> for information on the commonality of four-leaf clovers and tips for finding them (accessed January 15, 2025).
- <sup>13</sup>Y. Xiong, C. Bourgois, N. Sheremetyeva, W. Chen, D. Dahliah, H. Song, J. Zheng, S. M. Griffin, A. Sipahigil, and G. Hautier, "High-throughput identification of spin-photon interfaces in silicon," *Sci. Adv.* **9**, eadh8617 (2023).
- <sup>14</sup>Y. Xiong, J. Zheng, S. McBride, X. Zhang, S. M. Griffin, and G. Hautier, "Discovery of f center-like quantum defects in silicon," *arXiv:2405.05165* (2024).
- <sup>15</sup>V. Ivanov, A. Ivanov, J. Simoni, P. Parajuli, B. Kanté, T. Schenkel, and L. Tan, "Database of semiconductor point-defect properties for applications in quantum technologies," *arXiv:2303.16283* (2023).
- <sup>16</sup>J. C. Thomas, W. Chen, Y. Xiong, B. A. Barker, J. Zhou, W. Chen, A. Rossi, N. Kelly, Z. Yu, D. Zhou, S. Kumari, E. S. Barnard, J. A. Robinson, M. Terrones, A. Schwartzberg, D. F. Ogletree, E. Rotenberg, M. M. Noack, S. Griffin, A. Raja, D. A. Strubbe, G.-M. Rignane, A. Weber-Bargioni, and G. Hautier, "A substitutional quantum defect in WS<sub>2</sub> discovered by high-throughput computational screening and fabricated by site-selective STM manipulation," *Nat. Commun.* **15**, 3556 (2024).
- <sup>17</sup>F. Bertoldo, S. Ali, S. Manti, and K. S. Thygesen, "Quantum point defects in 2d materials—The QPOD database," *npj Comput. Mater.* **8**, 56 (2022).
- <sup>18</sup>J. Davidsson, F. Bertoldo, K. S. Thygesen, and R. Armiento, "Adsorption versus adsorption: High-throughput computation of impurities in 2d materials," *npj 2D Mater. Appl.* **7**, 26 (2023).
- <sup>19</sup>P. Huang, R. Lukin, M. Faleev, N. Kazeev, A. R. Al-Maceni, D. V. Andreeva, A. Ustyuzhanin, A. Tormasov, A. H. Castro Neto, and K. S. Novoselov, "Unveiling the complex structure-property correlation of defects in 2d materials based on high throughput datasets," *npj 2D Mater. Appl.* **7**, 6 (2023).
- <sup>20</sup>V. Ivády, J. Davidsson, N. T. Son, T. Ohshima, I. A. Abrikosov, and A. Gali, "Identification of Si-vacancy related room-temperature qubits in 4H silicon carbide," *Phys. Rev. B* **96**, 161114 (2017).
- <sup>21</sup>J. Davidsson, V. Ivády, R. Armiento, N. T. Son, A. Gali, and I. A. Abrikosov, "First principles predictions of magneto-optical data for semiconductor point defect identification: The case of divacancy defects in 4H-SiC," *New J. Phys.* **20**, 023035 (2018).
- <sup>22</sup>J. Davidsson, V. Ivády, R. Armiento, T. Ohshima, N. T. Son, A. Gali, and I. A. Abrikosov, "Identification of divacancy and silicon vacancy qubits in 6H-SiC," *Appl. Phys. Lett.* **114**, 112107 (2019).
- <sup>23</sup>J. Davidsson, "Theoretical polarization of zero phonon lines in point defects," *J. Phys. Condens. Matter* **32**, 385502 (2020).
- <sup>24</sup>J. Davidsson, "Color centers in semiconductors for quantum applications: A high-throughput search of point defects in SiC," Ph.D. thesis (Linköping University Electronic Press, 2021).
- <sup>25</sup>J. Davidsson, V. Ivády, R. Armiento, and I. A. Abrikosov, "ADAQ: Automatic workflows for magneto-optical properties of point defects in semiconductors," *Comput. Phys. Commun.* **269**, 108091 (2021).
- <sup>26</sup>R. Armiento, "Database-driven high-throughput calculations and machine learning models for materials design," in *Machine Learning Meets Quantum Physics, Lecture Notes in Physics*, edited by K. T. Schütt, S. Chmiela, O. A. von Lilienfeld, A. Tkatchenko, K. Tsuda, and K.-R. Müller (Springer International Publishing, Cham, 2020), Vol. 968.
- <sup>27</sup>G. Kresse and J. Hafner, "Ab initio molecular-dynamics simulation of the liquid-metal-amorphous-semiconductor transition in germanium," *Phys. Rev. B* **49**, 14251 (1994).
- <sup>28</sup>G. Kresse and J. Furthmüller, "Efficient iterative schemes for ab initio total-energy calculations using a plane-wave basis set," *Phys. Rev. B* **54**, 11169 (1996).
- <sup>29</sup>P. E. Blöchl, "Projector augmented-wave method," *Phys. Rev. B* **50**, 17953 (1994).
- <sup>30</sup>G. Kresse and D. Joubert, "From ultrasoft pseudopotentials to the projector augmented-wave method," *Phys. Rev. B* **59**, 1758 (1999).
- <sup>31</sup>J. P. Perdew, K. Burke, and M. Ernzerhof, "Generalized gradient approximation made simple," *Phys. Rev. Lett.* **77**, 3865 (1996).
- <sup>32</sup>B. Kramer and A. MacKinnon, "Localization: Theory and experiment," *Rep. Prog. Phys.* **56**, 1469 (1993).
- <sup>33</sup>B. Kaduk, T. Kowalczyk, and T. Van Voorhis, "Constrained density functional theory," *Chem. Rev.* **112**, 321–22077560 (2012).
- <sup>34</sup>M. L. Evans, J. Bergsma, A. Merkys, C. W. Andersen, O. B. Andersson, D. Beltrán, E. Blokhin, T. M. Boland, R. Castañeda Balderas, K. Choudhary, A. Díaz Díaz, R. Domínguez García, H. Eckert, K. Eimre, M. E. Fuentes Montero, A. M. Krajewski, J. J. Mortensen, J. M. Nápoles Duarte, J. Pietryga, J. Qi, F. d. J. Trejo Carrillo, A. Vaitkus, J. Yu, A. Zettl, P. B. de Castro, J. Carlsson, T. F. T. Cerqueira, S. Divilov, H. Hajiyani, F. Hanke, K. Jose, C. Oses, J. Riebesell, J. Schmidt, D. Winston, C. Xie, X. Yang, S. Bonella, S. Botti, S. Curtarolo, C. Draxl, L. E. Fuentes Cobas, A. Hospital, Z.-K. Liu, M. A. L. Marques, N. Marzari, A. J. Morris, S. P. Ong, M. Orozco, K. A. Persson, K. S. Thygesen, C. Wolverton, M. Scheidgen, C. Toher, G. J. Conduit, G. Pizzi, S. Gražulis, G.-M. Rignane, and R. Armiento, "Developments and applications of the OPTIMADE API for materials discovery, design, and data exchange," *Digit. Discov.* **3**, 1509 (2024).
- <sup>35</sup>J. Davidsson, R. Babar, D. Shafizadeh, I. G. Ivanov, V. Ivády, R. Armiento, and I. A. Abrikosov, "Exhaustive characterization of modified Si vacancies in 4H-SiC," *Nanophotonics* **11**, 4565 (2022).
- <sup>36</sup>C. Bradac, W. Gao, J. Forneris, M. E. Trusheim, and I. Aharonovich, "Quantum nanophotonics with group IV defects in diamond," *Nat. Commun.* **10**, 5625 (2019).
- <sup>37</sup>J. Davidsson, W. Stenlund, A. S. Parackal, R. Armiento, and I. A. Abrikosov, "Na in diamond: High spin defects revealed by the ADAQ high-throughput computational database," *npj Comput. Mater.* **10**, 109 (2024).
- <sup>38</sup>G. m. H. Thiering and A. Gali, "Ab initio magneto-optical spectrum of group-IV vacancy color centers in diamond," *Phys. Rev. X* **8**, 021063 (2018).
- <sup>39</sup>A. L. Falk, B. B. Buckley, G. Calusine, W. F. Koehl, V. V. Dobrovitski, A. Politi, C. A. Zorman, P. X.-L. Feng, and D. D. Awschalom, "Polytype control of spin qubits in silicon carbide," *Nat. Commun.* **4**, 1819 (2013).
- <sup>40</sup>M. Wagner, B. Magnusson, W. M. Chen, E. Jánzén, E. Sörman, C. Hallin, and J. L. Lindström, "Electronic structure of the neutral silicon vacancy in 4H and 6H SiC," *Phys. Rev. B* **62**, 16555 (2000).
- <sup>41</sup>O. Bulancea-Lindvall, J. Davidsson, I. G. Ivanov, A. Gali, V. Ivády, R. Armiento, and I. A. Abrikosov, "Temperature dependence of the AB lines and optical properties of the carbon-antisite-vacancy pair in 4H," *Phys. Rev. Appl.* **22**, 034056 (2024).
- <sup>42</sup>Originally there were 21,607 defects, but a bug created duplicates. After removing these duplicates, 8,450 unique defects remained.
- <sup>43</sup>O. Bulancea-Lindvall, J. Davidsson, R. Armiento, and I. A. Abrikosov, "Chlorine vacancy in 4H-SiC: An NV-like defect with telecom-wavelength emission," *Phys. Rev. B* **108**, 224106 (2023).
- <sup>44</sup>A. Jain, S. P. Ong, G. Hautier, W. Chen, W. D. Richards, S. Dacek, S. Cholia, D. Gunter, D. Skinner, G. Ceder, and K. A. Persson, "Commentary: The materials project: A materials genome approach to accelerating materials innovation," *APL Mater.* **1**, 011002 (2013).



- <sup>45</sup>S. Kanai, F. J. Heremans, H. Seo, G. Wolfowicz, C. P. Anderson, S. E. Sullivan, M. Onizhuk, G. Galli, D. D. Awschalom, and H. Ohno, "Generalized scaling of spin qubit coherence in over 12,000 host materials," *Proc. Natl. Acad. Sci. U. S. A.* **119**, e2121808119 (2022).
- <sup>46</sup>J. Davidsson, M. Onizhuk, C. Vorwerk, and G. Galli, "Discovery of atomic clock-like spin defects in simple oxides from first principles," *Nat. Commun.* **15**, 4812 (2024).
- <sup>47</sup>V. Somjit, J. Davidsson, Y. Jin, and G. Galli, "An NV-center in magnesium oxide as a spin qubit for hybrid quantum technologies," *npj Comput. Mater.* **11**, 74 (2025).
- <sup>48</sup>More defects in CaO due to inclusion of complexes up to fourth nearest neighbors.
- <sup>49</sup>A. M. Ferrenti, N. P. de Leon, J. D. Thompson, and R. J. Cava, "Identifying candidate hosts for quantum defects via data mining," *npj Comput. Mater.* **6**, 126 (2020).
- <sup>50</sup>O. Groppfeldt, J. Davidsson, and R. Armiento, "High-throughput exploration of NV-like color centers across host materials," *arXiv:2503.23828* (2025).
- <sup>51</sup>Ratio of NV-like defects lies somewhere from 1 in 600 (180 NV-like defects to 100,000 processed defects) to 1 in 60 (compared to ca 10,000 stable defects on the defect hull).
- <sup>52</sup>G. Abbas, O. Bulancea-Lindvall, J. Davidsson, R. Armiento, and I. A. Abrikosov, "Theoretical characterization of NV-like defects in 4H-SiC using ADAQ with scan and r2SCAN meta-GGA functionals," *Appl. Phys. Lett.* **126**, 154001 (2025).
- <sup>53</sup>I. Harris, C. J. Ciccarino, J. Flick, D. R. Englund, and P. Narang, "Group-III quantum defects in diamond are stable spin-1 color centers," *Phys. Rev. B* **102**, 195206 (2020).
- <sup>54</sup>H. von Bardeleben and J. Cantin, "NV centers in silicon carbide: From theoretical predictions to experimental observation," *MRS Commun.* **7**, 591–594 (2017).
- <sup>55</sup>T. Kobayashi, T. Shimura, and H. Watanabe, "Oxygen-vacancy defect in 4H-SiC as a near-infrared emitter: An ab initio study," *J. Appl. Phys.* **134**, 145701 (2023).
- <sup>56</sup>J. P. Goss, P. R. Briddon, M. J. Rayson, S. J. Sque, and R. Jones, "Vacancy-impurity complexes and limitations for implantation doping of diamond," *Phys. Rev. B* **72**, 035214 (2005).
- <sup>57</sup>Y. G. Zhang, Z. Tang, X. G. Zhao, G. D. Cheng, Y. Tu, W. T. Cong, W. Peng, Z. Q. Zhu, and J. H. Chu, "A neutral oxygen-vacancy center in diamond: A plausible qubit candidate and its spintronic and electronic properties," *Appl. Phys. Lett.* **105**, 052107 (2014).
- <sup>58</sup>J. Goss, R. Lowery, P. Briddon, and M. Rayson, "Density functional theory study of Al, Ga and In impurities in diamond," *Diamond Relat. Mater.* **142**, 110811 (2024).
- <sup>59</sup>F. J. Heremans, C. G. Yale, and D. D. Awschalom, "Control of spin defects in wide-bandgap semiconductors for quantum technologies," *Proc. IEEE* **104**, 2009 (2016).
- <sup>60</sup>V. Ivády, J. Davidsson, N. Deegan, A. L. Falk, P. V. Klimov, S. J. Whiteley, S. O. Hruszkewycz, M. V. Holt, F. J. Heremans, N. T. Son, D. D. Awschalom, I. A. Abrikosov, and A. Gali, "Stabilization of point-defect spin qubits by quantum wells," *Nat. Commun.* **10**, 5607 (2019).
- <sup>61</sup>W. Stenlund, J. Davidsson, R. Armiento, V. Ivády, and I. A. Abrikosov, "ADAQ-SYM: Automated symmetry analysis of defect orbitals," *Comput. Phys. Commun.* **308**, 109468 (2025).
- <sup>62</sup>D. Shafizadeh, J. Davidsson, T. Ohshima, I. A. Abrikosov, N. T. Son, and I. G. Ivanov, "Selection rules in the excitation of the divacancy and the nitrogen-vacancy pair in 4H- and 6H-SiC," *Phys. Rev. B* **109**, 235203 (2024).